

Positive strangeness contribution to the nucleon magnetic moment in a relativistic chiral potential model

X.B. Chen^{a,b}, X.S. Chen^{a,c}, Amand Faessler^c, Th. Gutsche^c, F. Wang^a

^aDepartment of Physics and Center for Theoretical Physics, Nanjing University, Nanjing 210093, China

^bDepartment of Physics, Changsha Institute of Electricity, Changsha 410077, China

^cInstitut für Theoretische Physik, Universität Tübingen, Auf der Morgenstelle 14, D-72076 Tübingen, Germany
(March 15, 2000)

The strangeness contribution to the nucleon magnetic moment is calculated at the one-loop level in a relativistic SU(3) chiral potential model and is found to be *positive*, that is, with an *opposite* sign to the nucleon strangeness polarization. It is the “Z” diagram that violates the usual relation between spin and magnetic moment. The positive value is due to the contribution from the intermediate excited quark states, while the intermediate ground state gives a negative contribution. Our numerical results agree quite well with the new measurement of the SAMPLE Collaboration.

PACS numbers: 12.39.Ki, 12.39.Fe, 12.39.Pn, 13.88.+e

The new determination of the strangeness magnetic form factor of the nucleon at $Q^2 = 0.1 \text{ GeV}^2$ by the SAMPLE collaboration [1] confirmed its previous result [2] and indicates a significantly *positive* value:

$$G_M^s(0.1 \text{ GeV}^2) = +0.61 \pm 0.17 \pm 0.21 \pm 0.19 \mu_N. \quad (1)$$

This result implies new challenges to our understanding of the nucleon structure since most theoretical calculations typically generate negative values for $\mu_s \equiv G_M^s(Q^2 = 0)$ (see [3,4] and references therein). A positive value for μ_s is also intuitively difficult to understand with respect to the usual magnetic moment-spin (μ - s) relation, since the strange quark polarization of the nucleon is confirmed to be *negative* both by experiments [5] and by lattice QCD calculations [6,7]. (Note that the negative charge of the strange quark has been extracted in the definition of G_M^s .)

In a recent paper [8], by using a relativistic chiral potential model, we have successfully reproduced the experimental result of the strange quark polarization (Δs) of the nucleon. In this paper we report on the corresponding result for the nucleon strangeness magnetic moment, especially in comparison to the nucleon strangeness polarization.

The nucleon magnetic moment μ_N is defined by its interaction with a static, external magnetic field \vec{B} :

$$\langle N | \sum_q -iQ_q \int d^3x \bar{\psi}_q \gamma^\mu \psi_q A_\mu | N \rangle \equiv -\vec{\mu}_N \cdot \vec{B}, \quad (2)$$

It can be shown that μ_N is related to the electromagnetic form factor by $\mu_N = \sum_q Q_q G_M^q(0)$ [9], where $G_M^q(k^2) \equiv F_1^q(k^2) + F_2^q(k^2)$ and F_1 and F_2 are defined through

$$\langle N | \bar{\psi}_q \gamma^\mu \psi_q | N \rangle = \bar{u}_N \left(F_1^q \gamma^\mu + \frac{i}{2M_N} F_2^q \sigma^{\mu\nu} k_\nu \right) u_N. \quad (3)$$

The contribution of the quark flavor q ($q = u, d, s$) to the nucleon magnetic moment is usually defined as

$\mu_q \equiv G_M^q(0)$. Equivalently, μ_q can be evaluated as the expectation value of the magnetic moment operator:

$$\mu_q = \langle N | \int d^3x \psi_q^\dagger (\vec{x} \times \vec{\alpha})_3 \psi_q | N \rangle, \quad (4)$$

which follows directly from Eq. (2) [10]. Eq. (4) is especially suitable for model calculations. In the following we will perform a perturbative calculation of μ_s in a chiral potential model.

Our starting point is the chiral Lagrangian

$$\begin{aligned} \mathcal{L} = & \bar{\psi}[i\cancel{\partial} - S(r) - \gamma^0 V(r)]\psi - \\ & \frac{1}{2F_\pi} \bar{\psi}[S(r)(\sigma + i\gamma^5 \lambda^i \phi_i) + (\sigma + i\gamma^5 \lambda^i \phi_i)S(r)]\psi + \\ & \frac{1}{2}(\partial_\mu \sigma)^2 + \frac{1}{2}(\partial_\mu \phi_i)^2 - \frac{1}{2}m_\sigma^2 \sigma^2 - \frac{1}{2}m_{\phi_i}^2 \phi_i^2. \end{aligned} \quad (5)$$

The model Lagrangian is derived from the σ model in which meson fields are introduced to restore chiral symmetry [11]. The flavor and color indices for the quark field ψ are suppressed; the scalar term $S(r) = cr + m$ represents the linear scalar confinement potential cr and the quark mass matrix m ; $V(r) = -\alpha/r$ is the Coulomb type vector potential and $F_\pi = 93 \text{ MeV}$ is the pion decay constant. σ and ϕ_i (i runs from 1 to 8) are the scalar and pseudoscalar meson fields, respectively and λ_i are the Gell-Mann matrices. The quark-meson interaction term of Eq.(5) is symmetrized since the mass matrix m does not commute with all λ_i for different quark masses.

At zeroth order the nucleon is described by the usual SU(6) three-quark ground state of the Hamiltonian

$$H_q = \int d^3x \psi^\dagger [\vec{\alpha} \cdot \frac{1}{i} \vec{\partial} + \beta S(r) + V(r)] \psi. \quad (6)$$

The lowest order contribution to μ_s arises from the one-loop diagrams of Fig. 1, which we now evaluate.

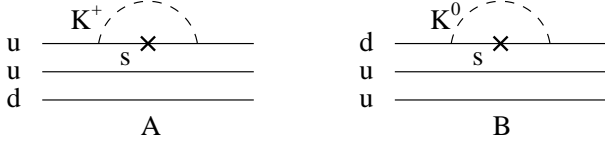


FIG. 1. Lowest order diagram for μ_s ; a cross on the quark line denotes the magnetic moment vertex $(\vec{x} \times \vec{\alpha})_3$.

The meson propagator, given by the Lagrangian of Eq. (5), is the free propagator. Since the non-perturbative confinement is included in H_q the quark propagator has to be obtained numerically, and in practise we have to work with time-ordered perturbation theory. We write the solution of H_q as

$$\psi(x) = \sum_{\alpha} u_{\alpha}(x) a_{\alpha} + \sum_{\beta} v_{\beta}(x) b_{\beta}^{\dagger}, \quad (7)$$

where $u_{\alpha}(x) = e^{-iE_{\alpha}t} u_{\alpha}(\vec{x}) \tau_{\alpha}$, $v_{\beta}(x) = e^{iE_{\beta}t} v_{\beta}(\vec{x}) \tau_{\beta}$; τ is the flavor wavefunction and the spatial wavefunction is:

$$u_{\alpha}(\vec{x}) = \left(\begin{array}{c} g_{njl}(r) \\ -i\vec{\sigma} \cdot \vec{r} f_{njl}(r) \end{array} \right) Y_{jl}^m(\hat{r}), \quad (8)$$

where g and f are real functions, n is the radial quantum number, and $Y_{jl}^m(\hat{r})$ are the vector spherical harmonics. For computational convenience, we will take the same form for $v_{\beta}(\vec{x})$.

In correspondence to Eq. (7), the quark propagator is

$$\begin{aligned} D(x_1, x_2) &\equiv \langle 0 | T \{ \psi(x_1), \bar{\psi}(x_2) \} | 0 \rangle \\ &= \theta(t_1 - t_2) \sum_{\alpha} u_{\alpha}(x_1) \bar{u}_{\alpha}(x_2) - \\ &\quad \theta(t_2 - t_1) \sum_{\beta} v_{\beta}(x_1) \bar{v}_{\beta}(x_2). \end{aligned} \quad (9)$$

Applying the propagators to Fig. 1, we get the contribution for a single quark line (with the initial and final states denoted as u_i and u_f , respectively):

$$\begin{aligned} \mu_s &= \frac{1}{F_{\pi}^2} \int d^4x_1 d^4x_2 \bar{u}_f(x_2) S(r_2) \gamma^5 \lambda^i \times \\ &\quad \left[\theta(t_2 - t) \theta(t - t_1) \sum_{\alpha\alpha'} u_{\alpha}(x_2) \Gamma_{\alpha\alpha'} \bar{u}_{\alpha'}(x_1) + \right. \\ &\quad \theta(t_1 - t) \theta(t - t_2) \sum_{\beta\beta'} v_{\beta}(x_2) \Gamma_{\beta\beta'} \bar{v}_{\beta'}(x_1) - \\ &\quad \theta(t_2 - t) \theta(t_1 - t) \sum_{\alpha\beta'} u_{\alpha}(x_2) \Gamma_{\alpha\beta'} \bar{v}_{\beta'}(x_1) - \\ &\quad \left. \theta(t - t_2) \theta(t - t_1) \sum_{\beta\alpha'} v_{\beta}(x_2) \Gamma_{\beta\alpha'} \bar{u}_{\alpha'}(x_1) \right] \times \\ &\quad S(r_1) \gamma^5 \lambda^i u_i(x_1) \frac{i}{(2\pi)^4} \int d^4k \frac{\delta_{ij} e^{-ik \cdot (x_1 - x_2)}}{k^2 - m_{\phi_i}^2 + i\epsilon}, \end{aligned} \quad (10)$$

where $\Gamma_{\alpha\alpha'} \equiv \int d^3x u_{\alpha}^{\dagger}(\vec{x} \times \vec{\alpha})_3 u_{\alpha'}$, and similarly for $\Gamma_{\beta\beta'}$ etc. The four time-ordered terms in Eq.(10) correspond to the time-ordered diagrams of Fig. 2.

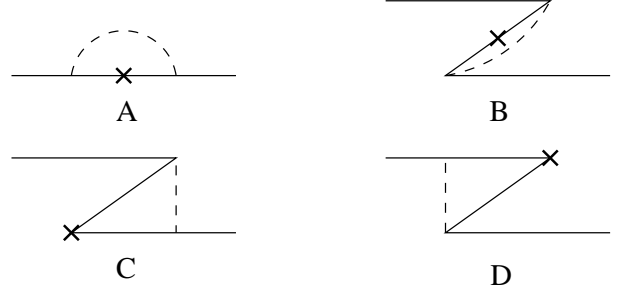


FIG. 2. Time-ordered diagrams of Fig. 1; A is the positive-energy state contribution; B is the negative-energy state contribution; C and D are the quark-antiquark pair creation and annihilation “Z” diagrams.

We omit here the details for the evaluation of μ_s of Eq. (10). The integrals of Eq. (10) can be reduced analytically to radial integrations at the vertex points (r_1 and r_2) and of the loop momentum $|\vec{k}|$. The remaining integrations are carried out numerically. To obtain μ_s for the whole nucleon, one still has to multiply a spin-isospin factor which can be straightforwardly calculated to be 2.

When calculating μ_s we allow strong variations of the model parameters entering in the Lagrangian of Eq. (5). Since $F_{\pi} = 93$ MeV and $m_K = 495$ MeV are fixed by experiment, our model contains four free parameters: the two quark masses $m_{u,d}$, m_s and the two strength constants of the scalar and vector potential denoted by c and α . The parameter α is fixed by the long-wavelength, transverse fluctuations of the QCD based static-source flux-tube picture [12,13]. It was obtained to be 0.26 in [14] and 0.30 in [15], while a much larger value of about 0.52 was used by the Cornell group [16]. Recent lattice calculation [17] got a value around 0.32 in the quenched approximation, and suggested that relaxing the quenched approximation may lead to $\alpha \sim 0.40$. Effective quark masses and confinement strength are rather uncertain quantities. We therefore choose in our calculation five different sets of parameters (see Table I), including both current and constituent quark masses.

TABLE I. Model parameters and the contribution to μ_s from the intermediate quark ground state only.

para. set	$m_{u,d}$ [MeV]	m_s [MeV]	α	c [GeV ²]	μ_s [μ_N] ground state
1	10	150	0.26	0.11	-0.0115
2	10	150	0.26	0.16	-0.0176
3	300	500	0.26	0.11	-0.0176
4	10	150	0.30	0.16	-0.0180
5	10	150	0.50	0.18	-0.0226

Fig. 3 gives the numerical results of μ_s in units of μ_N . The intermediate quark states are consistently summed up to a given energy. In the last column of Table I we list the contribution of the intermediate ground state. As evident from Fig. 3, for *all* choices of parameter sets, μ_s turns out to be *positive*, as long as enough excited quark states are taken into account. However, as already indicated in Table I the intermediate quark ground state always give a negative contribution. This explains why in many calculations at the baryon level, where the quarks are restricted to the ground state and the intermediate baryon is truncated to be the ground state octet or decuplet baryons, a negative value of μ_s is usually obtained.

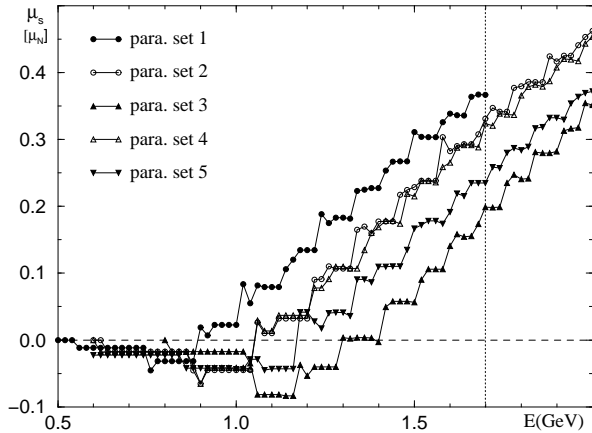


FIG. 3. Plot of μ_s as a function of the maximal energy up to which the intermediate states are summed.

We see in Fig. 3 that the summation over the quark intermediate states is divergent. This is because in the chiral Lagrangian of Eq. (5), the electromagnetic current of the strange quark is not separately conserved. To obtain a meaningful finite result, we must renormalize the composite, non-conserved magnetic moment operator of the strange quark. Analogous to the lattice renormalization, we cut the quark intermediate states at a certain energy, which should roughly correspond to the inverse of the lattice spacing ($a^{-1} \sim 1.7\text{GeV}$) in the lattice QCD calculation of nucleon properties [18]. The cutoff point is indicated in Fig. 3.

Fig. 3 shows that a larger quark mass or a stronger confinement (which is effectively a static mass) always reduce the magnetic moment, as expected. However, the variations of the vector potential do not affect μ_s too much.

To analyze how the positive value for μ_s arises, in Fig. 5 we give the separate contributions to μ_s from the time-ordered diagrams of Fig. 2 for the second set of parameters. Correspondingly in Fig. 6 we indicate the separate contributions of the time-ordered diagrams to strange quark polarization Δs of the nucleon [8].

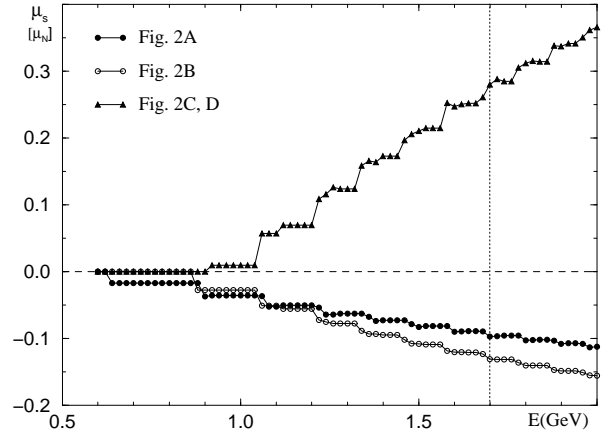


FIG. 4. Contributions to μ_s from the time-ordered diagrams of Fig. 2; the positive-energy and negative-energy states both generate a negative contribution, while the two “Z” diagrams yield a positive contribution. The results are given as a function of the energy cutoff on the intermediate quark states.

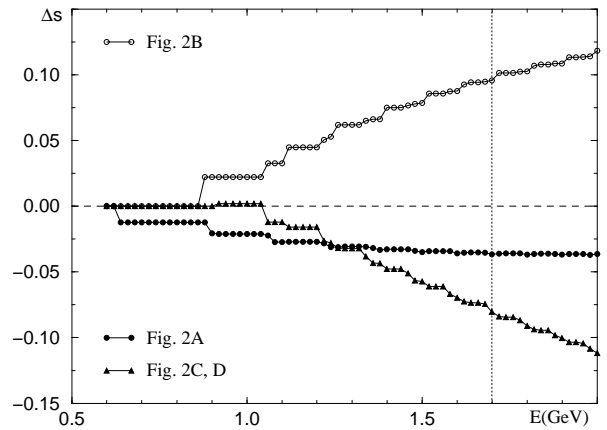


FIG. 5. Time-ordered diagrams' contributions to Δs ; the positive-energy, negative-energy states, and the “Z” diagrams give a negative, positive, and negative contribution, respectively. The results are given as a function of the energy cutoff on the intermediate quark states.

The results of Figs. 5 and 6 indicate why μ_s and Δs have opposite sign: the intermediate quark states give a contribution of the same sign (both negative) to μ_s and Δs , which is as expected; the antiquark states contribute a positive amount to Δs , but a negative amount to μ_s . This is also reasonable since the antiquark has an opposite charge to the quark. However, one would not expect the usual relation between spin and magnetic moment for the contributions from the “Z” diagrams in which a quark-antiquark pair is created or annihilated; an evident obstacle is that we do not know what sign of the charge we should attribute to these diagrams. Figs. 5

and 6 show that the “Z” diagrams give a negative contribution to the polarization while they generate a positive contribution to magnetic moment. They are also the dominating contributions (note that there are two “Z” diagrams); so eventually we get for the whole nucleon a negative strangeness polarization but a positive strangeness magnetic moment. This agrees well with the experimental results.

In summary, we found by a standard perturbative calculation that the SU(3) chiral potential model predicts a *positive* nucleon strangeness magnetic moment for a wide range of model parameters. Here the contributions from the intermediate excited states and the “Z” diagrams are most important. If one restricts the intermediate state to the quark ground state an opposite result is obtained. Further investigation of the time-ordered diagrams reveals that the positive-energy and negative-energy states (Figs. 2A and 2B) contribute to polarization and magnetic moment in the usual way that respects the relation between spin and magnetic moment; however this is not true for the “Z” diagrams, whose contribution is found to be dominant and therefore determines the overall sign of μ_s and Δs for the nucleon. Since in our calculations both for μ_s and Δs we have assumed only one Lagrangian, the success of our calculations can be regarded as a strong support of our approach and the chiral Lagrangian.

This work is supported by the CNSF (19675018), CSSED, CSSTC, the DFG (FA67/25-1), and the DAAD.

-
- [1] SAMPLE Collaboration (D.T. Spayde, *et al.*), Phys. Rev. Lett. **84**, 1106 (2000) (nucl-ex/9909010).
 - [2] SAMPLE Collaboration (B. Mueller, *et al.*), Phys. Rev. Lett. **78**, 3824 (1997).
 - [3] R.D. McKeown, in *Parity Violation in Atoms and Polarized Electron Scattering*, ed. by B. Frois and M.A.-Bouchiat, World Scientific, 423 (1999).
 - [4] S.J. Dong, K.F. Liu, and A.G. Williams, Phys. Rev. D **58**, 074504 (1998).
 - [5] For a review, see, e.g., U. Stiegler, Phys. Rep. **277**, 1 (1996).
 - [6] S.J. Dong, J.P. Lagae, and K.F. Liu, Phys. Rev. Lett. **75** 2096 (1995).
 - [7] M. Fukugita, Y. Kuramashi, M. Okawa, and A. Ukawa, Phys. Rev. Lett. **75** 2092 (1995).
 - [8] X.B. Chen, X.S. Chen, A. Faessler, T. Gutsche, F. Wang, hep-ph/0002200.
 - [9] See, e.g., S. Weinberg, *The Quantum Theory of Fields, Vol. I* (Cambridge University Press, 1995).
 - [10] See, e.g., T.D. Lee, *Particle Physics and Introduction to Field Theory* (Harwood Academic Publishers, 1981).
 - [11] See, e.g., A.W. Thomas, Advan. Nucl. Phys. **13**, 1 (1984).
 - [12] G. Parisi, R. Petronzio, F. Rapuano, Phys. Lett. B **128**, 418 (1983).
 - [13] J.D. Stack, Phys. Rev. D **29**, 1213 (1984).
 - [14] M. Luscher, Nucl. Phys. **B180**, 317 (1981).
 - [15] S. Itoh, Y. Iwasaki, T. Yoshie, Phys. Rev. D **33**, 1806, (1986).
 - [16] E. Eichten, K. Gottfried, T. Kinoshita, K.D. Lane, T.M. Yan, Phys. Rev. D **17**, 3090 (1978); Phys. Rev. D **21**, 203 (1980).
 - [17] G.S. Bali, K. Schilling, A. Wachter, Phys. Rev. D **56**, 2566 (1997).
 - [18] S.J. Dong, K.F. Liu, A.G. Williams, Phys. Rev. D **58**, 074504 (1998); S.J. Dong, J.F. Lagae, K.F. Liu, Phys. Rev. Lett. **75**, 2096 (1995).